⌘ *Author's Choice*

THE JOURNAL OF BIOLOGICAL CHEMISTRY VOL. 284, NO. 40, pp. 27273–27280, October 2, 2009

Apolipoprotein E4 Domain Interaction Induces Endoplasmic Reticulum Stress and Impairs Astrocyte Function*[S]

Received for publication, May 1, 2009, and in revised form, July 9, 2009 Published, JBC Papers in Press, August 7, 2009, DOI 10.1074/jbc.M109.014464

Ning Zhong[‡], Gayathri Ramaswamy[‡], and Karl H. Weisgraber[‡§¶1]

From the [‡]Gladstone Institute of Neurological Disease, San Francisco, California 94158 and the [§]Department of Pathology and [¶]Cardiovascular Research Institute, University of California, San Francisco, California 94143

Domain interaction, a structural property of apolipoprotein E4 (apoE4), is predicted to contribute to the association of apoE4 with Alzheimer disease. Arg-61 apoE mice, a gene-targeted mouse model specific for domain interaction, have lower brain apoE levels and synaptic, functional, and cognitive deficits. We hypothesized that domain interaction elicits an endoplasmic reticulum (ER) stress in astrocytes and an unfolded protein response that targets Arg-61 apoE for degradation. Primary Arg-61 apoE astrocytes had less intracellular apoE than wild-type astrocytes, and unfolded protein response markers OASIS (old astrocyte specifically induced substance), ATF4, and XBP-1 and downstream effectors were up-regulated. ER stress appears to cause global astrocyte dysfunction as glucose uptake was decreased in Arg-61 apoE astrocytes, and astrocyte-conditioned medium promoted neurite outgrowth less efficiently than wild-type medium in Neuro-2a cell cultures. We showed age-dependent up-regulation of brain OASIS levels and processing in Arg-61 apoE mice. ER stress and astrocyte dysfunction represent a new paradigm underlying the association of apoE4 with neurodegeneration.

Apolipoprotein (apo)[2] E4 is a major risk factor for Alzheimer disease (AD) and other forms of neurodegeneration, but the mechanisms are unknown (1, 2). ApoE4 is less effective than apoE3 in neuronal maintenance and injury repair, which may explain the increased risk (1). The basis for these isoform-specific differences must reflect differences in their structural properties (3, 4). One difficulty in linking a given structural property of apoE4 to the mechanisms or pathways associated with the higher risk for AD is that apoE4 differs from apoE3 and apoE2 in at least two ways; it has lower stability to protein unfolding with a greater tendency to form a molten globule state, and it exhibits domain interaction. Either or both of these structural properties could underlie the association of apoE4 with AD (3, 5, 6). From a mechanistic and therapeutic prospective, it is essential to single out the relative contributions of these structural features to neurodegeneration. This is impossible with currently available human apoE4 knock-in and transgenic mouse models, as they express all of the structural features of apoE4 simultaneously.

To circumvent this roadblock, we took advantage of the fact that wild-type (WT) mouse apoE does not exhibit apoE4 instability/molten globule formation or domain interaction. Therefore, we identified the amino acid differences in human apoE4 responsible for each of those structural features and "humanized" mouse apoE by introducing those residues into WT mouse *Apoe* (7, 8). To introduce domain interaction, we used gene targeting to generate Arg-61 apoE mice. These mice are a specific model of human apoE4 domain interaction, as mouse Arg-61 apoE exhibits this property but does not form a molten globule state (7, 8).

Previously, we demonstrated that, in the absence of stress (ischemia, trauma, amyloid-β protein toxicity, etc.), Arg-61 apoE mice have reduced levels of the synaptic proteins synaptophysin and neurolignin-1 in the brain, indicating neurodegeneration, and exhibit both functional synaptic deficits and memory deficits as a result of domain interaction (9). Domain interaction also resulted in lower levels of Arg-61 apoE in the brain, which were caused by reduced secretion of apoE by astrocytes and not by differential transcription (10). In this study, we demonstrate that in astrocytes, the major source of apoE in nonstressed brains (11), domain interaction in Arg-61 apoE is recognized as an abnormally folded protein by the endoplasmic reticulum (ER) protein quality control machinery. This recognition activates an ER stress response that affects astrocyte function and neuronal support.

EXPERIMENTAL PROCEDURES

Mice—Arg-61 apoE mice were generated as described and backcrossed with WT C57BL/6J mice for eight generations (8–10). Primary astrocyte cultures were dissociated from 3-day-old neonatal and 3-month-old adult mouse brains. Mice were housed and handled in accordance with the National Institutes of Health Guide for the Care and Use of Laboratory Animals.

* This work was supported, in whole or in part, by National Institutes of Health Grants PO1 AG022074 (to K. W.), RO1 AG20235 (to K. W.), and CO6 RR0118928 from the National Center for Research Resources. This work was also supported in part by American Health Assistance Foundation Pilot Grant for Alzheimer's Disease Research A2006-231 (to N. Z.), Alzheimer's Association Zenith Award AG028793 (to K. W.).

⌘ *Author's Choice*—Final version full access.

[S] The on-line version of this article (available at http://www.jbc.org) contains supplemental methods, Figs. 1 and 2, and Table 1.

[1] To whom correspondence should be addressed: Gladstone Institute of Neurological Disease, 1650 Owens St., San Francisco, CA 94158. Fax: 415-355-0824; E-mail: kweisgraber@gladstone.ucsf.edu.

[2] The abbreviations used are: apo, apolipoprotein; AD, Alzheimer disease; ER, endoplasmic reticulum; UPR, unfolded protein response; WT, wild-type; 2-NBDG, 2-[*N*-(7-nitobenz-2-oxa-1,3-diazol-4-yl)amino]-2-deoxy-D-glucose; ACM, astrocyte-conditioned medium; OASIS, old astrocyte specifically induced substance; PERK, PKR-like ER kinase; PKR, protein kinase R; PDI, protein disulfide isomerase; Herp, homocysteine-inducible ER protein; CHOP, C/EBP homologous protein; C/EBP, CCAAT-enhancer-binding protein; APP, amyloid precursor protein.

Primary Astrocyte Cultures—Neonatal astrocytes were cultured as described (10). Primary adult astrocyte cultures were prepared from the brains of 3-month-old WT, Arg-61 apoE, and apoE knock-out/WT heterozygous mice, according to published procedures with modifications (12). In brief, mouse brain cortex and hippocampus were dissected with a sterile razor blade and trypsinized for 20 min at 37 °C. Dissociated cells were filtered and suspended in fresh Dulbecco's modified Eagle's F-12 medium (Invitrogen) containing 10% fetal bovine serum, 1% penicillin-streptomycin, and 1% Primocin (Invitrogen). The cell suspensions were plated and cultured in Dulbecco's modified Eagle's F-12 medium at 37 °C in a 5% CO_2 atmosphere. To confirm that the cells were astrocytes, cultures were stained with a monoclonal antibody against intermediate filament glial fibrillary acidic protein. All cells were glial fibrillary acidic protein-positive under our culture conditions (see supplemental Fig. 1). Astrocytes from neonatal and 3-month-old mouse brains were used in quantitative real-time PCR experiments. Astrocytes from 3-month-old mouse brains were used in functional studies, as the transporter system matures in adult astrocytes.

Western Blot—Astrocyte intracellular levels of apoE and OASIS (old astrocyte specifically induced substance) and the brain levels of OASIS were quantitated by immunoblotting. Primary astrocyte cultures were grown to 80% confluence in 6-well plates, harvested, and lysed. Brain tissues were homogenized in ice-cold lysis buffer (50 mmol/liter Tris-HCl, pH 8.0, 150 mmol/liter NaCl, 0.1% SDS, 0.5% Nonidet P-40, 0.5% sodium deoxycholate, and a mixture of protease and phosphatase inhibitors) and centrifuged at 30,000 rpm for 30 min at 4 °C in a TLA 100.3 rotor in an Optima TL ultracentrifuge (Beckman Instruments). Supernatants from both cell lysate and brain homogenates were collected, and 25 μg of protein from each sample were analyzed by SDS-PAGE gel electrophoresis. OASIS was detected with an antibody against recombinant mouse OASIS peptide (1:10,000, Strategic Diagnostics, Newark, DE). The sensitivity and specificity of anti-OASIS antibody was tested (see supplemental methods and supplemental Fig. 2). Mouse WT apoE and Arg-61 apoE were detected with an antibody against recombinant, full-length WT mouse apoE (1:10,000). Protein bands were detected by chemiluminescence with horseradish peroxidase-coupled anti-rabbit IgG secondary antibody. The blots were scanned, and protein levels were quantitated by densitometry (ImageJ, National Institutes of Health, Bethesda, MD).

Quantitative Fluorogenic Real-time PCR—Total RNA from primary astrocyte cultures (over 80% confluence in T-75 flask) was isolated with RNeasy mini columns (Qiagen, Valencia, CA). Reverse transcription reactions (Applied Biosystems, Foster City, CA) contained 300 ng of DNase-treated total RNA and random hexamer and oligo(dT) primers (2.5 μM each) (see supplemental Table 1). Diluted reactions (6 ng of cDNA) were analyzed with SYBR green PCR reagents in duplicate on an ABI Prism 7700 sequence detector (Applied Biosystems). OASIS, ATF4, and XBP-1 mRNA levels and the mRNA levels of downstream effectors were determined relative to standard curves made with serial dilutions of pooled cDNAs (30, 6, and 1.2 ng) from all samples. Values were normalized to mouse 18 S RNA.

Fluorescence-activated Cell Sorting—Primary astrocytes were plated at a density of 5×10^4 cells/ml and cultured for 48 h. Cell viability or apoptosis was detected by the Vybrant apoptosis assay kit 2 (Molecular Probes). Apoptotic cells and dead cells were stained with Alexa Fluor 488-conjugated annexin V or propidium iodide and separated by fluorescence emission at 530 and >575 nm, respectively. Cell distribution was detected and analyzed by flow cytometry.

Glucose Uptake—Primary astrocytes were plated at 2500 cells/well in a 96-well plate and cultured for 48 h. Glucose uptake was detected with a fluorescent glucose derivative, 2-[*N*-(7-nitobenz-2-oxa-1,3-diazol-4-yl)amino]-2-deoxy-D-glucose (2-NBDG, Molecular Probes) (13, 14). The concentration of 2-NBDG and the incubation time were optimized for measurement of glucose uptake in primary astrocyte cultures. Intracellular 2-NBDG was measured with a microplate reader with excitation at 475 nm and emission 545 nm (13). The intracellular 2-NBDG fluorescence intensities were normalized to total cellular protein levels to avoid the bias from the different cell numbers.

Astrocyte-conditioned Medium—Primary astrocyte cultures (over 80% confluence in T-75 flask) were conditioned with serum-free Opti-MEM I medium for 48 h. The conditioned media from WT, Arg-61 apoE, and apoE knock-out/WT heterozygous mouse astrocytes were collected and filtered.

Neurite Outgrowth—Neuro-2a cells (American Type Culture Collection, Manassas, VA) were maintained at 37 °C in a humidified 5% CO_2 incubator in MEM containing 10% fetal bovine serum supplemented with nonessential amino acids, penicillin, and streptomycin. Neuro-2a cells were plated in 24-well plates at 12,000 cells/well. To induce neurite outgrowth, serum-containing medium was replaced with serum-free Opti-MEM I medium containing 50% astrocyte-conditioned medium (ACM). Neuro-2a cells were cultured in Opti-MEM I/ACM for 72 h, fixed, and stained with Coomassie Blue (Bio-Rad) to enhance visualization of cell bodies and neurites. Neurite outgrowth was quantified as the percentage of cells with neurites longer than 1× the cell body diameter.

Statistical Analysis—Quantitative data are expressed as mean ± S.E. Differences between two means were assessed with unpaired, two-tailed *t* tests. Differences among multiple means were evaluated by analysis of variance followed by a Tukey-Kramer *post hoc* test. For the age-dependent changes of OASIS levels, a two-way analysis of variance tested the effects of genotype and age.

RESULTS

Domain Interaction Results in Lower Levels of Intracellular Arg-61 ApoE in Primary Astrocytes

Previously, using WT and Arg-61 apoE mice and human apoE3 and apoE4 knock-in mice, we demonstrated that domain interaction results in lower levels of Arg-61 apoE and apoE4 than of WT mouse apoE and apoE3 in the brain, as reflected by reduced secretion and not differences in transcription (10). To determine whether Arg-61 apoE accumulated in astrocytes or was degraded, cell lysates were examined. In lysates of primary astrocyte cultures, Arg-61 apoE levels were 49.6 ± 3.8% ($p < 0.01$) lower than WT levels, indicating that Arg-61 apoE was targeted for degradation (Fig. 1).

Domain Interaction Up-regulates Unfolded Protein Response (UPR) Pathways

Next, we determined the levels of UPR components in primary astrocyte cultures by reverse transcription and real-time PCR. The levels of OASIS, an astrocyte-specific UPR transducer in the ATF6 (activating transcription factor) pathway (15), were 2.0 ± 0.2-fold higher in Arg-61 than in WT astrocytes, demonstrating transcriptional up-regulation (Fig. 2*A*). Expression of ATF4 and XBP-1 (X-box binding protein 1), components of two other common UPR pathways, PERK (PKR-like ER kinase) and IRE1 (inositol-requiring enzyme 1), were also up-regulated in Arg-61 astrocytes (1.3 ± 0.1- and 1.4 ± 0.2-fold higher than in WT astrocytes, respectively) (Fig. 2, *B* and *C*). Thus, domain interaction in Arg-61 apoE astrocytes elicited an ER stress response and activated all three UPR pathways.

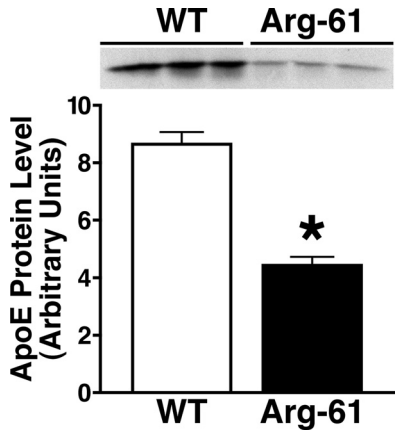

FIGURE 1. **ApoE levels in lysates of primary astrocytes from 3-day-old Arg-61 and WT apoE mice.** Lysates were analyzed by SDS-PAGE and Western blotting with an antibody against full-length mouse apoE. ApoE protein levels were quantitated by densitometry. *Error bars* represent S.E. $n = 9$ mice/group (*, $p < 0.01$ Arg-61 apoE mice *versus* WT).

Cleavage of Astrocyte OASIS in Response to ER Stress Induced by Domain Interaction

An ER stress response should result in cleavage of OASIS, generating an N-terminal fragment that is translocated to the nucleus, activating its target genes (16). Western blot analysis with an anti-OASIS antibody showed that OASIS was expressed as an ~80-kDa protein with minimal cleavage in WT astrocytes. However, in Arg-61 apoE astrocytes, a 55-kDa band was more prominent, demonstrating increased cleavage (Fig. 2*D*). Arg-61 astrocytes also expressed higher levels of OASIS protein, indicating that domain interaction induced ER stress and up-regulated UPR pathways. Total OASIS protein expression was 1.7 ± 0.2-fold higher in Arg-61 apoE astrocytes, which had higher levels of both full-length protein (Fig. 2*E*) and the 55-kDa fragment (Fig. 2*F*) (2.5 ± 0.1 *versus* WT 2.0 ± 0.1 and 1.9 ± 0.2 *versus* WT 1.2 ± 0.3 arbitrary units, respectively; both $p < 0.05$).

UPR Pathway Effectors Are Activated in Arg-61 ApoE Astrocytes

The cleaved cytosolic N-terminal fragment of OASIS is a transcription factor that, together with ATF4 and spliced XBP-1, increases the expression of genes encoding effectors of UPR pathways, including ER chaperones, such as BiP (immunoglobulin heavy chain binding protein) and GRP 94 (glucose-regulated protein 94), and proteins that catalyze protein folding, such as protein disulfide isomerases (PDIs) (17–19). BiP, GRP94, and PDI mRNA levels were 1.3 ± 0.1-, 1.4 ± 0.1-, and 1.3 ± 0.1-fold higher, respectively, in Arg-61 apoE astrocytes than WT; $p < 0.05$) (Fig. 3, *A*–*C*). mRNA levels of *GADD34* (growth arrest and DNA damage-inducible gene 34), which may protect against the destructive attenuation of translation mediated by PERK pathway activation (20), were also higher in Arg-61 apoE astrocytes (1.5 ± 0.2-fold, $p < 0.05$) (Fig. 3*D*).

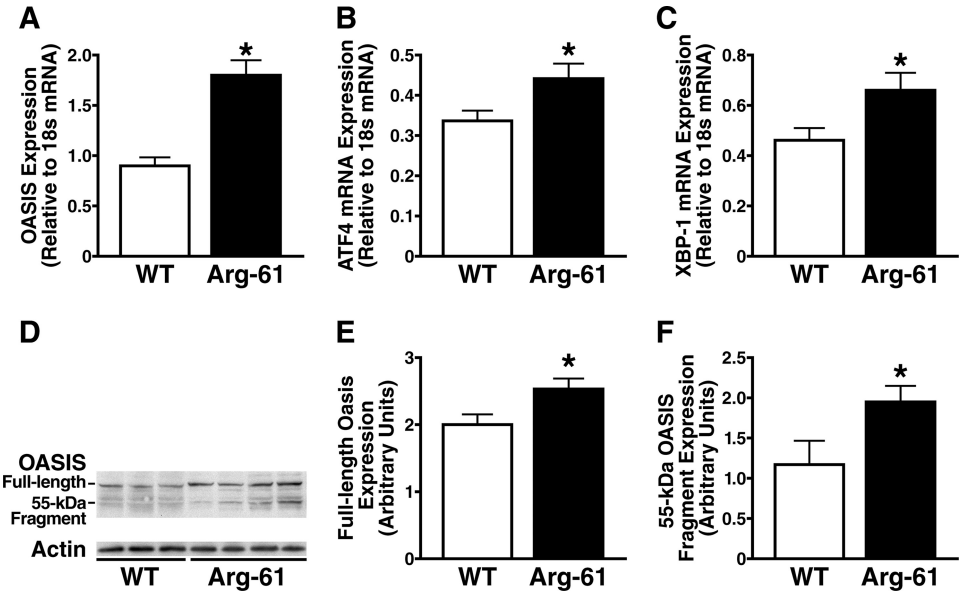

FIGURE 2. **UPR components are up-regulated in neonatal Arg-61 apoE astrocytes.** *A*–*C*, OASIS (*A*), ATF4 (*B*), and XBP-1 (*C*) mRNA levels were notably higher in Arg-61 apoE astrocytes than in WT astrocytes. OASIS was cleaved at the transmembrane region in response to ER stress induced by domain interaction in Arg-61 apoE astrocytes. *D*, expression of OASIS in primary astrocytes. Cell lysates from Arg-61 apoE and WT primary astrocytes were analyzed by Western blot with anti-OASIS antibody. Full-length OASIS appeared as a 80-kDa band in both WT and Arg-61 apoE astrocyte lysates. A 55-kDa band (cleaved OASIS fragment) appeared predominantly in Arg-61 apoE astrocytes. *E* and *F*, protein levels of full-length OASIS (*E*) and the 55-kDa OASIS fragment (*F*) were quantitated by densitometry ($n = 11$ WT mice and $n = 13$ Arg-61 apoE mice; *, $p < 0.05$ *versus* WT).

ER-associated degradation is one of the common response mechanisms. Homocysteine-inducible ER protein (Herp), an ER-resident membrane protein, was hypothesized to function for ER-associated degradation (21, 22). The mRNA level of Herp was 1.4 ± 0.2-fold higher in Arg-61 apoE astrocytes ($p < 0.05$) (Fig. 3*E*). CHOP (C/EBP homologous protein), a member of the C/EBP family of bZIP transcription factors, is expressed at high levels in response to ER stress and is believed to be a downstream effector in all three common UPR path-

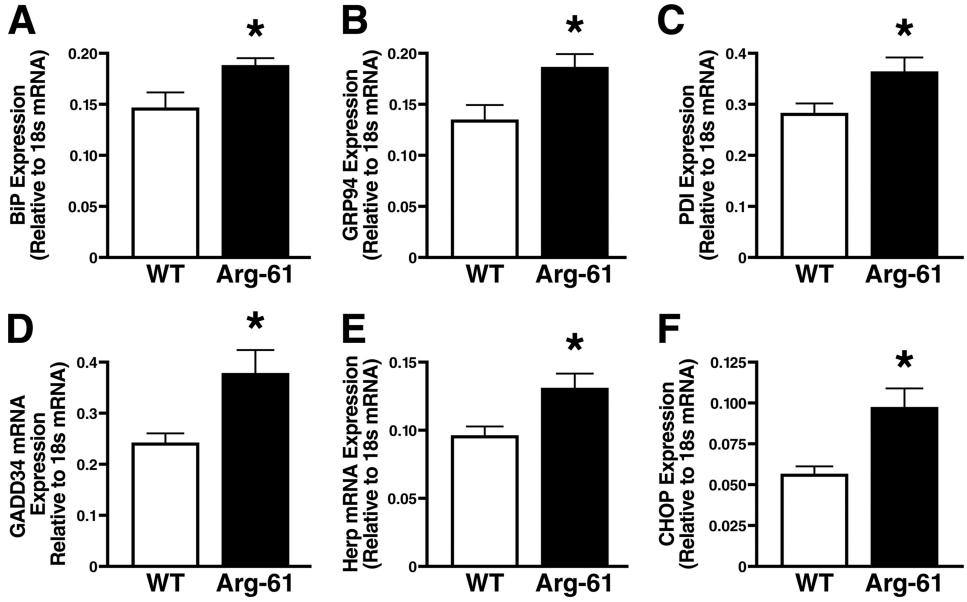

FIGURE 3. **Up-regulation of ER stress response and UPR downstream effectors.** mRNA levels of BiP (*A*), GRP94 (*B*), PDI (*C*), GADD34 (*D*), Herp (*E*), and CHOP (*F*) were determined by real-time PCR in neonatal Arg-61 apoE astrocytes ($n = 9$ mice/group; *, $p < 0.01$ *versus* WT).

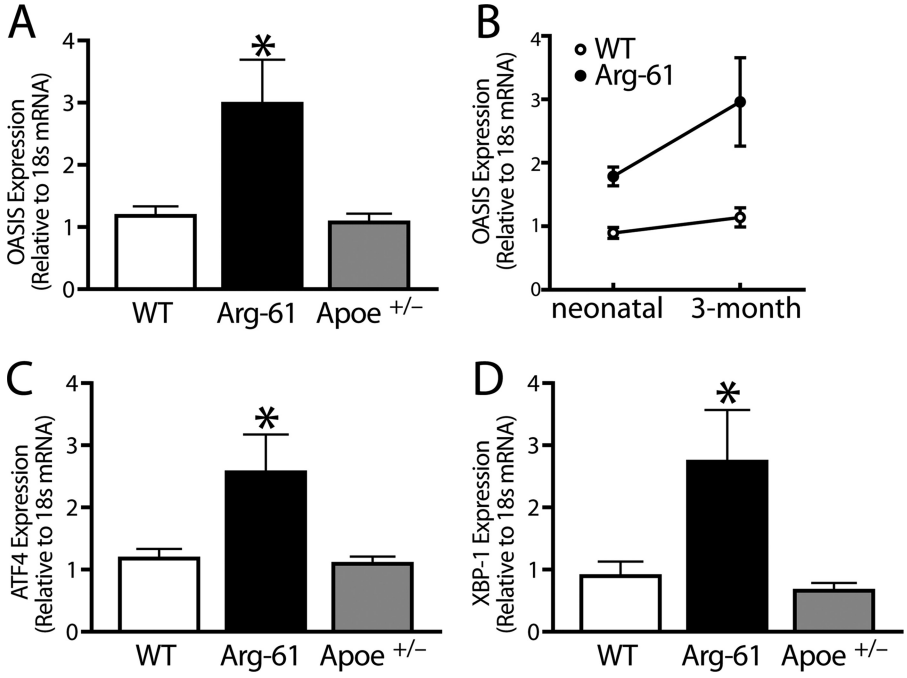

FIGURE 4. **UPR components were up-regulated in 3-month-old adult Arg-61 apoE astrocytes.** *A–D*, OASIS (*A* and *B*), ATF4 (*C*), and XBP-1 (*D*), mRNA levels were notably increased in Arg-61 apoE astrocytes. In $Apoe^{+/-}$ astrocytes, which had 50% lower apoE levels than WT astrocytes, UPR components were not up-regulated ($n = 8$ WT, $n = 6$ Arg-61 apoE, and $n = 7$ $Apoe^{+/-}$ mice; *, $p < 0.05$ *versus* WT for OASIS, XBP-1, and ATF4; *, $p > 0.05$ *versus* WT). *D*, the mRNA levels of OASIS were markedly elevated with ~70% more than Arg-61 apoE neonatal astrocytes (*, $p < 0.01$).

ways (23, 24). CHOP expression levels were 1.7 ± 0.2-fold higher ($p < 0.05$) in Arg-61 apoE astrocytes (Fig. 3*F*).

ER Stress Exists in Adult Arg-61 ApoE Astrocytes and Is Not Due to Lower ApoE Protein Levels

Previously, we showed that brain levels of Arg-61 apoE are lower than those of WT in E18 mouse embryos and remain lower up to 2 years of age (10). We, therefore, determined whether ER stress induced by domain interaction also existed in adult astrocytes. Indeed, mRNA levels of OASIS (Fig. 4*A*), ATF4 (Fig. 4*C*), and XBP-1 (Fig. 4*D*) were higher in cultures of astrocytes from adult (3-month-old) Arg-61 apoE mice (2.4 ± 0.6-, 2.2 ± 0.5-, and 3.1 ± 1.0-fold higher, respectively, than WT; $p < 0.05$).

A two-way analysis of variance test was used to determine whether there was an age effect on OASIS mRNA levels between the WT and Arg-61 apoE astrocytes from neonatal and adult brains. In WT adult astrocytes, OASIS mRNA levels were increased ~25% (Fig. 4*B*). However, age had a major effect on OASIS expression in Arg-61 apoE astrocytes. The mRNA levels of OASIS were markedly elevated with ~70% more than Arg-61 apoE neonatal astrocytes ($p < 0.01$, Fig. 4*B*), indicating that age-dependent expression of abnormally folded Arg-61 apoE exacerbates ER stress and UPR.

To rule out the possibility that the ER stress induced by domain interaction is due to the lower apoE protein levels, we examined astrocytes from 3-month-old heterozygous $Apoe^{+/-}$ mice, with 50% lower apoE levels. mRNA levels of OASIS, ATF4, and XBP-1 were not elevated (83 ± 10%, 92 ± 11%, and 72 ± 15% of WT levels, respectively, $p > 0.05$) (Fig. 4). Thus, simply reducing the apoE protein level is not sufficient to induce ER stress in primary astrocyte cultures, indicating a specific effect of Arg-61 apoE or domain interaction.

ER Stress Induced by Domain Interaction Causes Astrocyte Dysfunction

Cell Viability—Arg-61 apoE did not affect astrocyte viability or induce apoptosis. Flow cytometric analysis of primary cultures co-stained with Alexa Fluor 488-conjugated annexin V and propidium iodide showed no difference in the percentage of viable cells in WT (94.5 ± 0.8%) and Arg-61 apoE (93 ± 2.1%) astrocyte cultures ($p > 0.05$), and no apoptosis was detected (Fig. 5*A*).

Glucose Uptake—After a 2-min incubation with 2-NBDG (500 μM), a metabolic fluorescent marker of glucose uptake (13, 14, 25), Arg-61 apoE astrocytes had lower levels of fluorescence

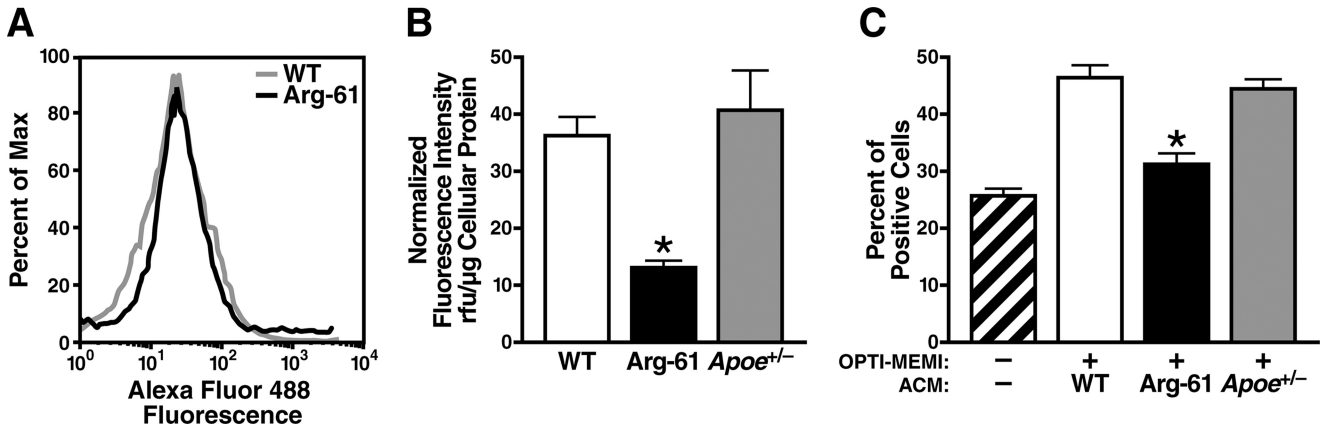

FIGURE 5. **Domain interaction in Arg-61 apoE astrocytes results in global astrocyte dysfunctions.** *A*, cell viability was not different in Arg-61 apoE and WT astrocytes, and no apoptosis or cell death was detected. *Max*, maximum. *B*, glucose uptake was lower in Arg-61 apoE astrocytes than WT (*, $p < 0.05$ *versus* WT), but the reduction of apoE levels by 50% in $Apoe^{+/-}$ astrocytes did not affect the glucose uptake in astrocytes ($n = 8$ WT, $n = 8$ Arg-61 apoE, and $n = 7$ $Apoe^{+/-}$ mice). *rfu*, relative light units. *C*, ACM from Arg-61 apoE astrocytes was less efficient in promoting neurite outgrowth in Neuro-2a cells than WT ACM (*, $p < 0.01$ *versus* WT). $Apoe^{+/-}$ ACM was sufficient to support neurite outgrowth ($n = 6$ mice/group).

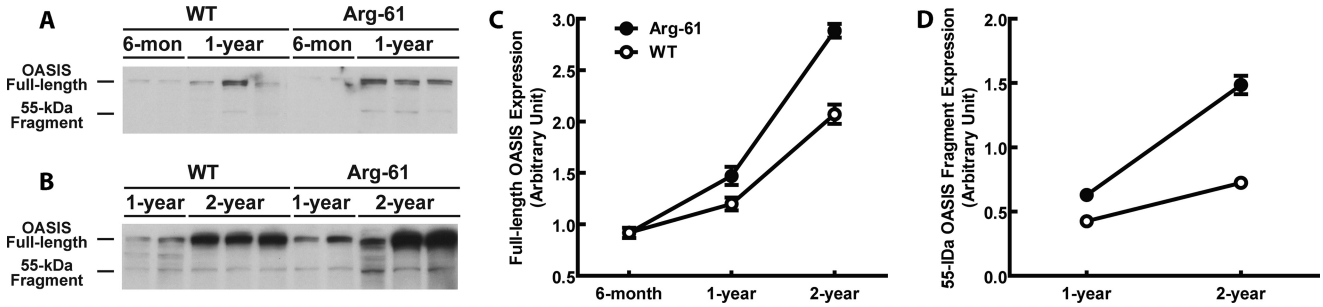

FIGURE 6. **Expression of OASIS in the brains of 6-month- and 1- and 2-year-old mice and age-dependent up-regulation of brain OASIS protein levels and processing in Arg-61 apoE mice.** *A* and *B*, full-length OASIS appeared as an 80-kDa band in both WT and Arg-61 apoE brain homogenates from different age groups. *B*, a 55-kDa band (cleaved OASIS fragment) appeared predominantly in Arg-61 apoE mouse brains. *C* and *D*, quantitation of OASIS expression and processing. Densitometry was used to quantitate protein levels of full-length OASIS (*C*) and the 55-kDa OASIS fragment (*D*) in brain samples from 1- and 2-year-old mice ($n = 6$ 6-month, $n = 9$ 1-year, and $n = 11$ 2-year-old mice). The cleaved OASIS and full-length OASIS protein levels were markedly increased in both 1-year-old and 2-year-old Arg-61 apoE mouse brains ($p < 0.05$ *versus* WT).

than WT astrocytes (13.4 ± 0.8 *versus* 36.2 ± 3.2 normalized relative fluorescence units; $p < 0.05$) (Fig. 5*B*).

Neurite Outgrowth—The percentage of Neuro-2a cells with neurite outgrowth in serum-free medium was 26 ± 2.0%. To compare the abilities of Arg-61 apoE and WT astrocytes to support neurite outgrowth, we incubated Neuro-2a cells with ACM from Arg-61 apoE astrocytes and WT astrocytes for 48 h. Arg-61 apoE ACM was less effective at promoting neurite outgrowth than WT apoE ACM, as shown by the lower percentage of cells with neurites (31 ± 4.8% *versus* 46 ± 4.8%, $p < 0.01$) (Fig. 5*C*).

Astrocyte Dysfunction Is Not Due to a Lower Level of ApoE or Cholesterol

To examine the effect of apoE levels on glucose uptake and neurite outgrowth, we examined $Apoe^{+/-}$ astrocytes (50% reduction in apoE and cholesterol) and ACM from these cells. Glucose uptake was not impaired in $Apoe^{+/-}$ astrocytes (Fig. 5*B*), and $Apoe^{+/-}$ ACM supported neurite outgrowth (Fig. 5*C*). Thus, the adverse deficiencies in Arg-61 apoE astrocytes were not due to the lower levels of apoE or cholesterol.

Domain Interaction Up-regulates Astrocyte-specific OASIS Protein Expression and Cleavage in Vivo

To determine whether ER stress also occurs in Arg-61 apoE mice, we assessed OASIS protein expression in brain homogenates of 6-month-old and 1- and 2-year-old mice by immunoblotting. Because cleavage of full-length OASIS induces activation of an ER stress response, we also examined the amounts of full-length (80-kDa) and cleaved (55-kDa fragment) OASIS in WT and Arg-61 apoE mice.

At 6 months of age, full-length OASIS was expressed at similar low levels in both WT and Arg-61 mouse brains (Fig. 6, *A* and *B*, $p > 0.05$ *versus* WT) with no detectable cleavage. In 1-year-old WT brains, levels of full-length OASIS were increased about 30%, and 36 ± 1.9% of the protein was cleaved. The percentage of cleaved OASIS (43 ± 1.8%) was significantly higher in 1-year-old Arg-61 mouse brains ($p < 0.05$ *versus* WT), and full-length OASIS protein levels were increased 60% ($p < 0.05$ *versus* WT).

Age itself is a brain stressor and a risk factor for AD. Although we noticed a further increase of full-length OASIS levels in aged (2-year-old) WT mouse brains, the percentage of cleaved fragments remained similar (35 ± 1.2%) to that of 1-year-old WT brains, demonstrating no further OASIS processing. However, both full-length OASIS protein levels (96% increase from 1-year levels, $p < 0.01$ *versus* WT, Fig. 6, *B* and *C*) and cleavage (Fig. 6, *B* and *D*) were markedly increased in 2-year-old Arg-61 mouse brains. The percentage of cleaved OASIS increased to 52 ± 2.1% ($p < 0.01$ *versus* WT), indicating an increased and constitutively active ER stress response in

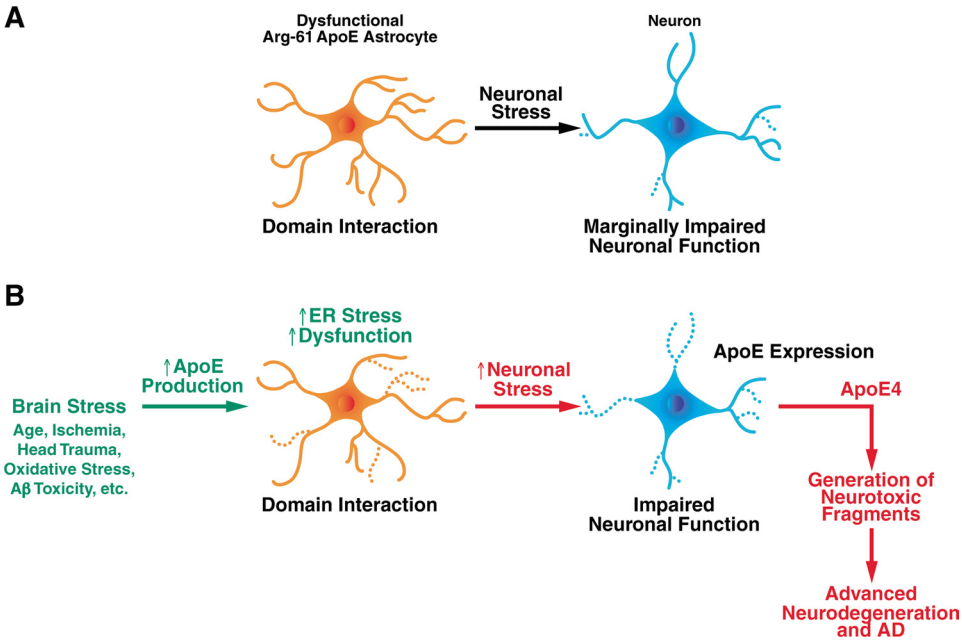

FIGURE 7. **Role of astrocyte ER stress in neurodegeneration and AD.** *A*, Arg-61 apoE domain interaction induces astrocyte dysfunction, resulting in less effective neuronal maintenance. *B*, as the effects of stress accumulate over time, astrocytes are signaled to express additional apoE for neuronal repair. This exacerbates ER stress and further compromises astrocyte support. Lacking support from astrocytes, stressed neurons begin to express apoE to repair themselves. In the case of apoE4, this leads to the generation of neurotoxic fragments, leading to more extensive neuronal damage and degeneration and ultimately to AD.

aged Arg-61 mouse brains due to domain interaction. The age-dependent, astrocyte-specific up-regulation of OASIS protein levels and processing in Arg-61 apoE mice correlates with our previous observation of an age-dependent loss of the synaptic vesicle protein, synaptophysin, indicating that age-dependent and astrocyte-specific ER stress in Arg-61 apoE mice has an impact on global brain functions (9).

DISCUSSION

Using the Arg-61 apoE domain interaction mouse model to determine the effect of domain interaction on astrocytes and their function, we demonstrated that domain interaction induces an ER stress response and activates the three common UPR pathways, IRE1, PERK, and OASIS. In addition, several UPR downstream effector genes were up-regulated. Furthermore, the ER stress response and UPR adversely affected Arg-61 apoE astrocyte functions, as demonstrated by reduced glucose uptake and reduced support for neuronal neurite outgrowth. Finally, consistent with the cell culture studies, the protein levels of OASIS and its processing were increased in aged Arg-61 apoE mouse brains, indicating an age-dependent, astrocyte-specific stress response *in vivo*. These results reveal a novel role for astrocytes in apoE4-mediated neurodegeneration.

Until recently, astrocytes were considered to be an inert support scaffold for neurons and their interactions (26). However, astrocytes are now appreciated for exerting a major influence on the extracellular environment and are essential for glial-neuronal interactions, which are believed to be critical in mechanisms of neurodegenerative diseases (27–29).

Normally, secreted proteins such as apoE are correctly folded, modified, and assembled in the ER. Within the ER, smooth transit of proteins to the cis-Golgi is monitored and assisted by an elaborate quality control process, which includes chaperones and folding enzymes (30). When misfolded or abnormally folded proteins are recognized and accumulate in the ER, the cell activates a signaling response that up-regulates UPR pathways (17, 18, 20, 31).

In this study, we demonstrated that Arg-61 apoE does not accumulate intracellularly in astrocytes, suggesting that it is targeted for degradation. Recent pulse-chase studies confirm this possibility (32). Degradation of Arg-61 apoE suggests that domain interaction is recognized as an abnormally folded protein in the ER, eliciting an ER stress response and activating three common UPR pathways. Most important in the case of domain interaction is the age-dependent astrocyte-specific up-regulation and increased processing (cleavage) of OASIS in both Arg-61 apoE astrocyte cultures and mouse brains, clearly demonstrating an astrocyte-specific constitutive ER stress *in vitro* and *in vivo*. Signaling from the stress-sensing proteins initially activates the cellular processes to protect the cell. Ultimately, it promotes cell injury with a chronic ER stress response (23, 24, 33). Although not specifically associated with astrocytes, ER stress and dysfunction are believed to be linked to the pathogenesis of several neurological and neurodegenerative diseases, including AD (34–37).

The chronic ER stress response has the potential to globally impair the function of astrocytes, compromising their ability to support and maintain neurons, by sequestering chaperones or reducing protein translation. Consistent with this possibility, glucose uptake by Arg-61 apoE astrocytes was impaired, suggesting a metabolic defect. Interestingly, positron emission tomography studies in humans have shown glucose hypometabolism in nondemented apoE4 carriers as young as their mid-twenties (38–42). Glucose metabolism examined in positron emission tomography studies actually reflects astrocyte function (13, 43), suggesting that the hypometabolism in nondemented apoE4 carriers is due to decreased glucose uptake by astrocytes. In addition, ACM from Arg-61 apoE astrocytes was less effective in promoting neurite outgrowth, which indicates impaired ability to support synaptogenesis and neuronal repair. Together, these results demonstrate that domain interaction and the associated ER stress have a global effect on astrocyte function. Chronic ER stress in astrocytes might suppress the expression and activity of glial glutamate transporters and affect the balance of glutamate homeostasis (44). Consistent with this possibility, we previously found that levels of astrocyte-specific glutamate transporter, GLT1, are reduced in Arg-61 apoE mouse brains, indicating an *in vivo* astrocyte dys-

function and a possible excitotoxic effect (9). It is reasonable to speculate that activated chronic ER stress responses in Arg-61 apoE astrocytes results in decreased GLT1 expression and activity, thus linking astrocyte ER stress and dysfunction to a chronic glutamate excitotoxicity (44). Chronic glutamate excitotoxicity is believed to be one of the mechanisms in the pathogenesis of a range of neurodegenerative diseases, including AD (45). All of these effects could contribute to the synaptic, functional, and cognitive deficits that we have identified in the Arg-61 apoE model (9).

Astrocytes are the major source of apoE in nonstressed brains to support and maintain normal neuronal functions (11). Because astrocytes play critical roles in many brain functions, even a slight impairment could eventually compromise the response to further stress and contribute to the phenotype in these mice and to neurological disease in humans (Fig. 7). Our present findings support the conclusion that astrocytes contribute more directly, in the absence of ischemia, trauma and amyloid-β protein toxicity, to the association of apoE4 with neurodegenerative diseases, possibly also including AD.

A potential scenario is that apoE4 domain interaction impairs the ability of astrocytes to support neuronal function over a lifetime (Fig. 7). Early in life in the absence of brain stress, Arg-61 apoE astrocytes exert a low level of ER stress response, as evidenced by low OASIS protein levels and minimal OASIS cleavage in 6-month-old Arg-61 apoE mouse brains. This indicates that young Arg-61 apoE astrocytes can sufficiently maintain the protein quality control machinery and astrocyte function to support neuronal function *in vivo* (Fig. 7*A*). As the effects of stress accumulate over time, from aging, ischemia, oxidative stress, head trauma, or antibody toxicity, astrocytes are called upon to express additional apoE for neuronal repair. With WT apoE, the increased demand for apoE does not elicit a significant ER stress, as shown by no further increase in OASIS processing as animals age. In marked contrast, with Arg-61 apoE, ER stress is exacerbated (Fig. 7*B*), as shown by the prominent age-dependent up-regulation of OASIS brain levels and increased OASIS cleavage in Arg-61 apoE mice. Therefore, Arg-61 apoE astrocyte support of neurons becomes more compromised and even less effective. Consistent with this scenario is our observation that synaptophysin brain levels in Arg-61 apoE mice at 6 months are identical to WT, but at 12 months, the levels are significantly reduced and further decline at 24 months (9). Without the necessary support from astrocytes, stressed neurons begin to express apoE and try to support themselves, as demonstrated previously (11). In the case of apoE4, this leads to the generation of neurotoxic C-terminal-truncated fragments and more extensive neuronal damage and degeneration, setting up a destructive cycle that ultimately leads to AD (1, 46–49) (Fig. 7*B*). Alternatively, compromised neurons may be more susceptible to the recently described death receptor 6/APP pathway that activates caspase-dependent programs, leading to axon pruning and neuronal death (50). Another possibility is a shift in APP processing to generation of APP fragments that lead to neuronal death resulting from an imbalance in signal transduction (51). These scenarios, all potentially initiated by astrocyte dysfunction, represent a potential explanation for the greater risk and lower age of onset of AD in apoE4 carriers (49).

Our findings in Arg-61 apoE mice suggest that domain interaction is a therapeutic target in AD and other neurodegenerative diseases. Proof of principle for an approach to target domain interaction by converting apoE4 into an apoE3-like molecule has been established (52). In addition, it is clear that AD is a multifactorial disease. Several pathways and processes that have been implicated in AD are downstream of astrocyte influence (29). Therefore, astrocytes are ideally positioned to impact multiple pathways simultaneously, at least in apoE4 carriers, who constitute ~65–80% of AD patients. Thus, targeting the reduction of astrocyte ER stress represents another potentially important therapeutic strategy.

Acknowledgments—We thank Belinda Cabriga for excellent technical assistance, John Carroll and Chris Goodfellow for graphics, Stephen Ordway and Gary Howard for editorial assistance, and Linda Turney for manuscript preparation.

REFERENCES

1. Mahley, R. W., Weisgraber, K. H., and Huang, Y. (2006) *Proc. Natl. Acad. Sci. U.S.A.* **103,** 5644–5651
2. Huang, Y. (2006) *Neurology* **66,** Suppl. 1, S79–S85
3. Hatters, D. M., Peters-Libeu, C. A., and Weisgraber, K. H. (2006) *Trends Biochem. Sci.* **31,** 445–454
4. Zhong, N., and Weisgraber, K. H. (2009) *J. Biol. Chem.* **284,** 6027–6031
5. Morrow, J. A., Hatters, D. M., Lu, B., Hochtl, P., Oberg, K. A., Rupp, B., and Weisgraber, K. H. (2002) *J. Biol. Chem.* **277,** 50380–50385
6. Dong, L. M., and Weisgraber, K. H. (1996) *J. Biol. Chem.* **271,** 19053–19057
7. Hatters, D. M., Peters-Libeu, C. A., and Weisgraber, K. H. (2005) *J. Biol. Chem.* **280,** 26477–26482
8. Raffai, R. L., Dong, L. M., Farese, R. V., Jr., and Weisgraber, K. H. (2001) *Proc. Natl. Acad. Sci. U.S.A.* **98,** 11587–11591
9. Zhong, N., Scearce-Levie, K., Ramaswamy, G., and Weisgraber, K. H. (2008) *Alzheimers Dement.* **4,** 179–192
10. Ramaswamy, G., Xu, Q., Huang, Y., and Weisgraber, K. H. (2005) *J. Neurosci.* **25,** 10658–10663
11. Xu, Q., Bernardo, A., Walker, D., Kanegawa, T., Mahley, R. W., and Huang, Y. (2006) *J. Neurosci.* **26,** 4985–4994
12. Lin, D. T., Wu, J., Holstein, D., Upadhyay, G., Rourk, W., Muller, E., and Lechleiter, J. D. (2007) *Neurobiol. Aging* **28,** 99–111
13. Loaiza, A., Porras, O. H., and Barros, L. F. (2003) *J. Neurosci.* **23,** 7337–7342
14. Yamada, K., Saito, M., Matsuoka, H., and Inagaki, N. (2007) *Nat. Protoc.* **2,** 753–762
15. Kondo, S., Murakami, T., Tatsumi, K., Ogata, M., Kanemoto, S., Otori, K., Iseki, K., Wanaka, A., and Imaizumi, K. (2005) *Nat. Cell Biol.* **7,** 186–194
16. Murakami, T., Kondo, S., Ogata, M., Kanemoto, S., Saito, A., Wanaka, A., and Imaizumi, K. (2006) *J. Neurochem.* **96,** 1090–1100
17. Ron, D., and Walter, P. (2007) *Nat. Rev. Mol. Cell Biol.* **8,** 519–529
18. Bernales, S., Papa, F. R., and Walter, P. (2006) *Annu. Rev. Cell Dev. Biol.* **22,** 487–508
19. Zhang, K., and Kaufman, R. J. (2004) *J. Biol. Chem.* **279,** 25935–25938
20. Rutkowski, D. T., and Kaufman, R. J. (2004) *Trends Cell Biol.* **14,** 20–28
21. Kokame, K., Agarwala, K. L., Kato, H., and Miyata, T. (2000) *J. Biol. Chem.* **275,** 32846–32853
22. Ma, Y., and Hendershot, L. M. (2004) *J. Biol. Chem.* **279,** 13792–13799
23. Xu, C., Bailly-Maitre, B., and Reed, J. C. (2005) *J. Clin. Invest.* **115,** 2656–2664
24. Oyadomari, S., and Mori, M. (2004) *Cell Death Differ.* **11,** 381–389
25. Leira, F., Louzao, M. C., Vieites, J. M., Botana, L. M., and Vieytes, M. R. (2002) *Toxicol. in Vitro* **16,** 267–273

26. Volterra, A., and Meldolesi, J. (2005) *Nat. Rev. Neurosci.* **6,** 626–640
27. Maragakis, N. J., and Rothstein, J. D. (2006) *Nat. Clin. Pract. Neurol.* **2,** 679–689
28. Seifert, G., Schilling, K., and Steinhäuser, C. (2006) *Nat. Rev. Neurosci.* **7,** 194–206
29. Barres, B. A. (2008) *Neuron* **60,** 430–440
30. Hol, E. M., and Scheper, W. (2008) *J. Mol. Neurosci.* **34,** 23–33
31. Schröder, M., and Kaufman, R. J. (2005) *Annu. Rev. Biochem.* **74,** 739–789
32. Riddell, D. R., Zhou, H., Atchison, K., Warwick, H. K., Atkinson, P. J., Jefferson, J., Xu, L., Aschmies, S., Kirksey, Y., Hu, Y., Wagner, E., Parratt, A., Xu, J., Li, Z., Zaleska, M. M., Jacobsen, J. S., Pangalos, M. N., and Reinhart, P. H. (2008) *J. Neurosci.* **28,** 11445–11453
33. Zhang, K., and Kaufman, R. J. (2006) *Neurology* **66,** S102–S109
34. Forman, M. S., Lee, V. M., and Trojanowski, J. Q. (2003) *Trends Neurosci.* **26,** 407–410
35. Rao, R. V., and Bredesen, D. E. (2004) *Curr. Opin. Cell Biol.* **16,** 653–662
36. Zhao, L., and Ackerman, S. L. (2006) *Curr. Opin. Cell Biol.* **18,** 444–452
37. Wu, J., and Kaufman, R. J. (2006) *Cell Death Differ.* **13,** 374–384
38. de Leon, M. J., Convit, A., Wolf, O. T., Tarshish, C. Y., DeSanti, S., Rusinek, H., Tsui, W., Kandil, E., Scherer, A. J., Roche, A., Imossi, A., Thorn, E., Bobinski, M., Caraos, C., Lesbre, P., Schlyer, D., Poirier, J., Reisberg, B., and Fowler, J. (2001) *Proc. Natl. Acad. Sci. U.S.A.* **98,** 10966–10971
39. Lee, K. U., Lee, J. S., Kim, K. W., Jhoo, J. H., Lee, D. Y., Yoon, J. C., Lee, J. H., Lee, D. S., Lee, M. C., and Woo, J. I. (2003) *J Neuropsychiatry Clin. Neurosci.* **15,** 78–83
40. Reiman, E. M., Caselli, R. J., Chen, K., Alexander, G. E., Bandy, D., and Frost, J. (2001) *Proc. Natl. Acad. Sci. U.S.A.* **98,** 3334–3339
41. Reiman, E. M., Chen, K., Alexander, G. E., Caselli, R. J., Bandy, D., Osborne, D., Saunders, A. M., and Hardy, J. (2005) *Proc. Natl. Acad. Sci. U.S.A.* **102,** 8299–8302
42. Small, G. W., Mazziotta, J. C., Collins, M. T., Baxter, L. R., Phelps, M. E., Mandelkern, M. A., Kaplan, A., La Rue, A., Adamson, C. F., Chang, L., Guze, B. H., Corder, E. H., Saunders, A. M., Haines, J. L., Pericak-Vance, M. A., and Roses, A. D. (1995) *JAMA* **273,** 942–947
43. Nehlig, A., and Coles, J. A. (2007) *GLIA* **55,** 1238–1250
44. Markowitz, A. J., White, M. G., Kolson, D. L., and Jordan-Sciutto, K. L. (2007) *Cellscience* **4,** 111–146
45. Masliah, E., Alford, M., DeTeresa, R., Mallory, M., and Hansen, L. (1996) *Ann. Neurol.* **40,** 759–766
46. Mahley, R. W., Huang, Y., and Weisgraber, K. H. (2007) *Curr. Alzheimer Res.* **4,** 537–540
47. Mahley, R. W., and Huang, Y. (2006) *Acta Neurol. Scand. Suppl.* **185,** 8–14
48. Huang, Y. (2006) *Curr. Opin. Drug Discov. Devel.* **9,** 627–641
49. Huang, Y., Weisgraber, K. H., Mucke, L., and Mahley, R. W. (2004) *J. Mol. Neurosci.* **23,** 189–204
50. Nikolaev, A., McLaughlin, T., O'Leary, D. D., and Tessier-Lavigne, M. (2009) *Nature* **457,** 981–989
51. Bredesen, D. E. (2009) *Mol. Neurodegener.* **4,** 27
52. Ye, S., Huang, Y., Müllendorff, K., Dong, L., Giedt, G., Meng, E. C., Cohen, F. E., Kuntz, I. D., Weisgraber, K. H., and Mahley, R. W. (2005) *Proc. Natl. Acad. Sci. U.S.A.* **102,** 18700–18705